Article

Dramatic Steric Behavior in Electron Transfer from Various Donors to CFBr

Peter W. Harland, and Philip R. Brooks

J. Am. Chem. Soc., **2003**, 125 (43), 13191-13197• DOI: 10.1021/ja036451b • Publication Date (Web): 07 October 2003

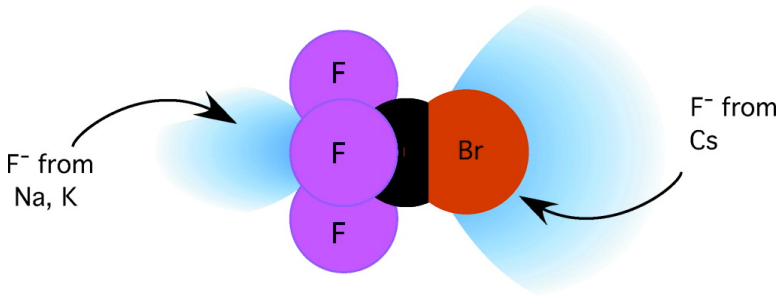

More About This Article

Additional resources and features associated with this article are available within the HTML version:

- Supporting Information
- Links to the 1 articles that cite this article, as of the time of this article download
- Access to high resolution figures
- Links to articles and content related to this article
- Copyright permission to reproduce figures and/or text from this article

View the Full Text HTML

J|A|C|S
ARTICLES
Published on Web 10/07/2003

Dramatic Steric Behavior in Electron Transfer from Various Donors to CF_3Br

Peter W. Harland† and Philip R. Brooks*

Contribution from the Chemistry Department and Rice Quantum Institute, Rice University, Houston, Texas 77251

Received May 31, 2003; E-mail: brooks@python.rice.edu

Abstract: Different alkali metal atoms are observed to donate electrons to CF_3Br molecules that are oriented in space. For collision energies high enough to overcome the Coulomb attraction, a positive ion/negative ion pair is observed and mass-analyzed using coincident time-of-flight mass spectroscopy. The alkali metal cation and various negative ions are observed. The most abundant negative ion is the bromide ion, Br^-, formed preferentially by attack at the Br end of the molecule. The steric asymmetry to produce Br^- is almost identical for all of the alkali metal donors. Fluoride ions are formed in smaller abundance and reflect completely different behavior among the donors. Sodium and potassium have high thresholds and prefer the CF_3 end of the molecule, whereas cesium prefers the Br end of the molecule. Sodium and potassium apparently interact with the transient CF_3Br^- molecular negative ion while it is in the process of decomposing.

I. Introduction

Chemical bonds are made by electrons being shared between atoms.[1] It should thus really come as no surprise that electron transfer is an important step in forming chemical bonds.[2−6] This transfer is normally assumed to be a tunneling process between the neutral donor/acceptor pair (D/A) and the charge-transfer pair, D^+/A^-. This will be facilitated if the potential energy surfaces intersect, because then the electron can be transferred in a Franck−Condon process without moving the nuclei. This crossing normally occurs at elevated energies, requiring activation of the D/A pair to have a geometry equivalent to the D^+/A^- product, which must then be collisionally deactivated. These activating and deactivating processes are enormously important in solution, and the role of the solvent in activating the reagents is so important that it can overwhelm subtle details of the transfer.[7]

To study the actual electron transfer without competition from other processes, we isolate the event in a single collision between neutral particles in molecular beams. The collision process can distort the neutral molecule, making it possible to form a transient molecular negative ion in a geometry potentially different from that of the neutral molecule. These negative ions are likely to be different from those traditionally formed by electron bombardment.[8−13] Bombardment with a free electron necessarily requires electrons with kinetic energy greater than zero and produces a transient negative ion (with the unstable geometry of the neutral) which has too much energy to be stable.[14] This transient ion will thus lose the extra electron (autodetach) or break apart into fragments. The transient molecular negative ion is unlikely to be collisionally stabilized, except in solution, because autodetachment can occur on femtosecond time scales[15] and fragmentation can occur on the subpicosecond time scales of molecular vibrations.

In electron-transfer collisions between fast atoms and molecules, on the other hand, the atomic core acts as a "solvent" to activate and deactivate the system. The fate of the electron acceptor (fragmentation vs stabilization), and the degree to which these experiments can mimic those in solution, depends on how effectively the electron donor relaxes the transient molecular negative ion. Most early studies[16−18] were confined to a single donor atom, usually Na or Cs, and, in a few cases where donors were compared, only relatively minor differences were found.[19−22]

† Present address: Chemistry Department, University of Canterbury, Christchurch, New Zealand.

(1) Lewis, G. N. *J. Am. Chem. Soc.* **1916**, *38*, 762.
(2) Ashby, E. C. *Acc. Chem. Res.* **1988**, *21*, 414−21.
(3) Jedlinski, Z. *Acc. Chem. Res.* **1998**, *31*, 55−61.
(4) Yamataka, H.; Aida, M.; Dupuis, M. *Chem. Phys. Lett.* **1999**, *300*, 583−7.
(5) Glukhovtsev, M. N.; Pross, A.; Schlegel, H. B.; Bach, R. D.; Radom, L. *J. Am. Chem. Soc.* **1996**, *118*, 11258−64.
(6) Bakken, V.; Danovich, D.; Shaik, S.; Schlegel, H. B. *J. Am. Chem. Soc.* **2001**, *123*, 130−4.
(7) Marcus, R. A. *Angew. Chem.* **1993**, *32*, 1111−1122.
(8) Cooper, C. D.; Compton, R. N. *J. Chem. Phys.* **1974**, *60*, 2424−9.
(9) Stockdale, J. A.; Davis, F. J.; Compton, R. N.; Klots, C. E. *J. Chem. Phys.* **1974**, *60*, 4279.
(10) Tang, S. Y.; Rothe, E. W.; Reck, G. P. *Int. J. Mass Spectrom. Ion Phys.* **1974**, *14*, 79−88.
(11) Tang, S. Y.; Mathur, B. P.; Rothe, E. W.; Reck, G. P. *J. Chem. Phys.* **1976**, *64*, 1270−5.
(12) Compton, R. N.; Cooper, C. D. *J. Chem. Phys.* **1977**, *66*, 4325−29.
(13) Harris, S. A.; Wiediger, S. D.; Brooks, P. R. *J. Phys. Chem.* **1999**, *103*, 10035−41.
(14) Massey, H. S. W. *Negative Ions*; Cambridge University Press: New York, 1976.
(15) Schulz, G. J. *Rev. Mod. Phys.* **1973**, *43*, 423−486.
(16) Los, J.; Kleyn, A. W. In *Ion-Pair Formation*; Davidovits, P., McFadden, D. L., Eds.; Academic Press: New York, 1979; pp 279−330.
(17) Lacmann, K. *Adv. Chem. Phys.* **1980**, *30*, 513−583.
(18) Kleyn, A. W.; Los, J.; Gislason, E. A. *Phys. Rep.* **1982**, *90*, 1−71.
(19) Compton, R. N.; Reinhardt, P. W.; Cooper, C. D. *J. Chem. Phys.* **1975**, *63*, 3821−7.
(20) Compton, R. N.; Reinhardt, P. W.; Cooper, C. D. *J. Chem. Phys.* **1978**, *68*, 4360−7.
(21) Cooper, C. D.; Frey, W. F.; Compton, R. N. *J. Chem. Phys.* **1978**, *69*, 2367−74.

Atoms in high Rydberg states can also be used as donors,[23] and negative ion formation is observed to be exquisitely sensitive to the quantum number.[24] Atoms with very high quantum numbers can donate an electron at distances so large that the electron appears to be a "free" electron. Atoms with intermediate lower quantum numbers (higher ionization potentials) must approach more closely before the electron can be transferred, and the nascent positive ion is observed to affect the electron attachment process.[25]

In the present experiments, the molecular beam environment allows us to react several different alkali metal atoms with CF_3Br molecules oriented in space. CF_3Br can easily be oriented, produces both Br^- and F^-, and is known to form a stable molecular negative ion. The dominant product ion is Br^-, and, after the energy deficit was corrected for, the steric behavior is essentially identical for all of the alkali metals. In contrast, fluoride ion production depends on the donor: Cs collisions prefer the positive end of CF_3Br, but Na and K prefer the negative end. All of the cesium processes favor the positive end of the molecule, suggesting that the electron is almost "free", with little interaction from the Cs^+ core. The differences in the steric preference for formation of F^- show that Na^+ and K^+ can significantly interact with the transient CF_3Br^- ion.

II. Experimental Section

The apparatus has been described in several earlier papers.[13,26] Beams of fast atoms are generated by charge-exchange.[27] Alkali metal atoms are ionized on a hot tungsten filament inside a stainless steel oven, accelerated toward a grounded slit, and then they drift in a field-free region inside the oven to undergo resonant charge-transfer collisions with neutral atoms. Charged deflection plates mounted outside the oven remove any residual ions so the beam consists only of neutral species. Space charge effects severely diminish the intensity at low energies.

Beams of CF_3Br are formed by supersonic expansion of He mixtures ($X_{He} = 0.9$) and are directed along the axis of an inhomogeneous hexapole electrostatic field 1.6 m long. The rotational temperature of the CF_3Br is estimated to be about 5 K.[28] The electrostatic field contains no obstacles, and a weak beam is transmitted even if no voltage is applied to the hexapole rods. Applying a high voltage (HV, typically ±10 kV) to the hexapole rods causes an interaction W between the field and molecule

$$W = -\mu \cdot E = -\mu EMK/(J(J+1)) = -\mu E\langle\cos\theta\rangle$$

where J, K, and M are the rotational state quantum numbers,[29] and θ is the angle between the top axis and the field. Molecules with $\langle\cos\theta\rangle < 0$ are deflected toward the field axis, thereby focusing the molecules and increasing their intensity. Molecule in states with $\langle\cos\theta\rangle = 0$ are undeflected. A small number in the weak beam transmitted at HV = 0 having $\langle\cos\theta\rangle > 0$ are attracted toward the rods and defocused, but this effect is overwhelmed by the number of molecules which focus.[30−33] The beam intensity for symmetric top molecules thus drastically increases when high voltage (HV) is applied to the rods.

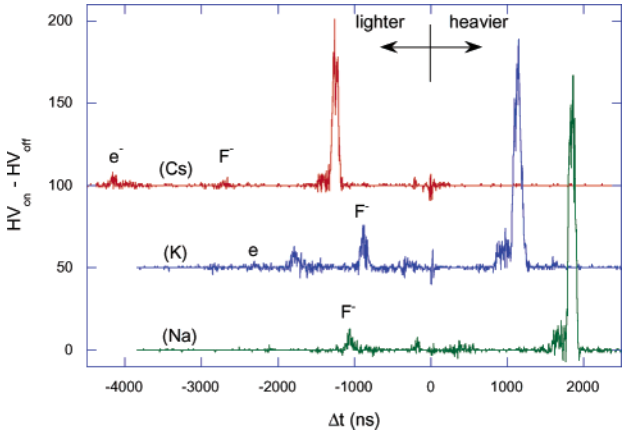

Figure 1. Representative coincidence TOF spectra for CF_3Br reacting with Cs, K, and Na after subtracting HV_{off} signals (CF_3 end, $E_{CM} = 5.8$, 14, and 9.5 eV for Cs, K, and Na). Large peaks are Br^-.

The beams cross at right angles between two identical time-of-flight (TOF) mass spectrometers inside an ultrahigh vacuum chamber. Weak fields are impressed along the flight path between the hexapole and the beam crossing to ensure that the molecules remain in the same J, K, and M states.[34] Collisions occur in the weak (~300 V/cm) field between the mass spectrometers, and the molecules are oriented in this field with the positive end of the molecule pointing toward the positive field plate. One TOF mass spectrometer detects positive ions and the other detects negative ions, and the field between the TOF mass spectrometers defines the direction of orientation of the molecules. Reversing the polarities of the mass spectrometers reverses the field and the orientation.

Transfer of an electron from the alkali metal to the CF_3Br molecule produces a positive ion/negative ion pair, and both of these ions can be detected if the available energy, E, is enough to overcome the Coulomb attraction of the ions, $E >$ (IP + BDE − EA). The ionization potentials of the alkali metal atom and negative ion product are IP and −EA, respectively, and BDE is the bond dissociation energy of any bonds broken. Because the beams are continuous and the TOF voltages are constant, there is no time zero for a time-of-flight measurement. Yet the positive and the negative ions are made simultaneously, so they have the same time zero. We measure the difference in flight times, and this is sufficient to determine the mass of the negative ion because the distances and mass of the positive ion are known. Observed time differences for known ions are used to calibrate the mass spectrum, and this calibration agrees with that calculated from known distances and voltages[13] to within about 3%.

Figure 1 shows representative flight time differences for the three systems studied here. The signal from the positive ion is used to start a time-to-digital converter (TDC), and the TDC stop is supplied by the signal from the negative ion, delayed 4 μs for Na and K and 7 μs for Cs. This delay ensures that all negative ions and electrons arrive at the TDC after the positive ion start signal and has been subtracted from the measured values of Δt, resulting in the negative values in the figure. Negative ions with the same mass as the alkali metal would appear at $\Delta t = 0$, and the spikes apparent here are noise. Ions heavier than the alkali metal appear at $\Delta t > 0$, and lighter ions appear at $\Delta t < 0$.

The coincidence spectra shown in Figure 1 are the difference between spectra taken with HV on and those with HV off. With HV on, the

(22) Baede, A. P. M.; Auerbach, D. J.; Los, J. *Physica* **1972**, *64*, 134−48.
(23) Dunning, F. B.; Stebbings, R. F. *Annu. Rev. Phys. Chem.* **1982**, *33*, 173−89.
(24) Desfrançois, C.; Périquet, V.; Lyapustina, S. A.; Lippa, T. P.; Robinson, D. W.; Bowen, K. H.; Nonaka, H.; Compton, R. N. *J. Chem. Phys.* **1999**, *111*, 4569−76.
(25) Kalamarides, A.; Marawar, R. W.; Ling, X.; Walter, C. W.; Lindsay, B. G.; Smith, K. A.; Dunning, F. B. *J. Chem. Phys.* **1990**, *92*, 1672−6.
(26) Harris, S. A.; Harland, P. W.; Brooks, P. R. *Phys. Chem. Chem. Phys.* **2000**, *2*, 787−91.
(27) Helbing, R. K. B.; Rothe, E. M. *Rev. Sci. Instrum.* **1968**, *39*, 1948.
(28) Wiediger, S. D.; Harland, P. W.; Holt, J. R.; Brooks, P. R. *J. Phys. Chem. A* **1998**, *102*, 1112−1118.
(29) Townes, C. H.; Schawlow, A. L. *Microwave Spectroscopy*; Dover: New York, 1975.
(30) Brooks, P. R. *Science* **1976**, *193*, 11−16.
(31) Parker, D. H.; Bernstein, R. B. *Annu. Rev. Phys. Chem.* **1989**, *40*, 561−595.
(32) Loesch, H. J. *Annu. Rev. Phys. Chem.* **1995**, *46*, 555−94.
(33) Brooks, P. R.; Harland, P. W. In *Effect of Molecular Orientation on Electron Transfer and Electron Impact Ionization*; Adams, N. G., Babcock, L. M., Eds.; JAI Press: Greenwich, CT, 1996; Vol. 2, pp 1−39.
(34) Brooks, P. R.; Jones, E. M.; Smith, K. *J. Chem. Phys.* **1969**, *51*, 3073.

Table 1. Apparent Threshold Voltages (eV)[a]

	Cs	K	Na
T_{Br}	3.6 (0.1)	4.0 (0.1)	4.6 (0.1)
T_F	3.6 (0.1)	8.6 (0.1)	9.8 (0.2)
T_e	3.6 (0.1)	7.5 (0.1)	8.5 (0.1)
T_{Br}^{calc}	3.52	3.97	4.77
T_F^{calc}	5.57	6.02	6.82
IP[36]	3.89	4.34	5.14

[a] EA:[36] (F) = 3.40; (Br) = 3.37. BDE:[36] (C−F) = 5.08; (C−Br) = 2.99. T_X^{calc} = IP − EA(X) + BDE(C−X).

signal is from state-selected molecules oriented in the field plus a minor contribution from randomly oriented molecules that would have passed through the hexapole with the HV off. This random contribution is removed by subtracting the HV_{off} signals. The HV off signal arises from truly randomly oriented molecules and is used to normalize any differences in ion collection and detection efficiency between the two detectors.[35] To change the orientation, the extant electric field must be reversed, which requires that the TOF voltages must be swapped. The negative ion TOF mass spectrometer becomes the positive ion mass spectrometer, and vice versa. A computer controls the hexapole voltage, detector polarity, and kinetic energy for comparison between orientations. Data are taken at different energies chosen at random for each run to avoid any systematic bias in the results.

III. Results

As suggested by Figure 1, all three donor atoms produce Br^- as the major ion, with minor contributions from F^- and electrons. Very small signals are observed at m/e = 149 corresponding to the molecular negative ion, CF_3Br^-.

Energy Calibration. Occasional modifications to the electrode geometry inside the fast atom beam source make it necessary to calibrate the energy scales for different alkali metals. An iterative process using the Br^- thresholds accomplishes this calibration as follows: a nominal CM threshold is determined using uncorrected accelerating voltages. Comparison with thresholds calculated using known values determines a correction to the lab energy, which is then used to redetermine the CM threshold. The final energy scale includes a small correction for speed of the CF_3Br. Thresholds for the other ions are determined after this calibration and are shown in Table 1.

Despite the small daily variations in signal arising from variations in beam intensities, the data for each of the alkali metals yield, within experimental error, the same threshold for positive/negative end attack in agreement with our earlier conclusions for CH_3Br.[13] The Br^- thresholds are forced to agree with known values to within ∼0.1 eV, and values shown in parentheses are the difference between positive and negative attack. These apparent thresholds are uncertain by ∼0.5 eV because the threshold is enormously sensitive to very small signals and the energy spread of the beams is not taken into account.

Negative Ions Formed. The most abundant negative ion for all of the donor atoms was Br^-, and Figure 2 shows the signal rate for Br^- ions obtained with HV on for positive end attack. Negative end (CF_3 end) attack, shown only for sodium, is less productive for all alkali metals. The signal rates depend on both the CF_3Br intensity (constant except for daily variations) and the alkali metal beam intensities, which are determined by different operating conditions. The large signals for cesium could thus reflect a high Cs beam intensity or a high cross section for reaction. While the reactive cross sections for cesium is probably the largest, the alkali metal beam intensity differences can be accounted for by scaling the potassium and sodium data. Figure 2 shows that these scaled data almost coincide with the cesium data. These signals thus have the same energy dependence and suggest that the processes responsible for the production of Br^- are the same for all of the donors.

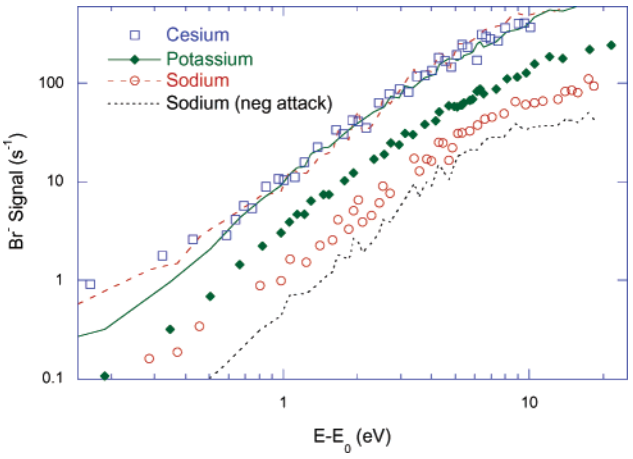

Figure 2. Positive end Br^- signals (HV on) plotted versus energy above threshold, ($E - E_0$), for the three alkali metals. (E_0 is the experimental Br threshold after calibration.) Curves through the cesium data represent the potassium data and sodium data scaled by factors of 3.0 and 8.0, respectively. Dotted line shows Br^- formed from negative end attack with sodium.

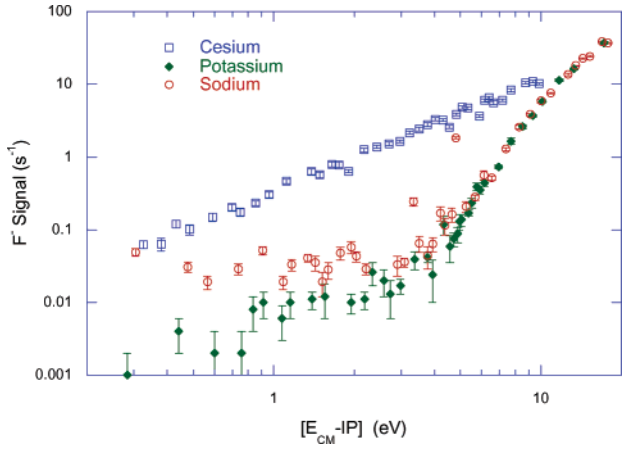

Figure 3. F^- signal rates for HV on, positive end attack versus (E_{CM} − IP) for the three alkali metals.

The HV_{on} signal rates for electrons and F^- for positive end attack are shown in Figures 3 and 4. In these figures, the signal rates are plotted against the energy above the ionization potential of the alkali metal atom. It is clear that, while potassium and sodium behave similarly, cesium is completely different. Thus, the ion formation processes must be similar for sodium and potassium, but different for cesium. Negative end attack signals are essentially the same on these log scales and are omitted for clarity.

Further insight into this difference is gained by plotting the fractions of electrons and F^- as a function of energy for the three alkali metal atom donors in Figures 5 and 6. Cesium interactions produce electrons and F^- in fractions that are essentially energy independent, whereas the potassium and sodium fractions are strongly and similarly dependent on energy. Data are for

(35) Brooks, P. R.; Harris, S. A. *J. Chem. Phys.* **2002**, *117*, 4220−32.

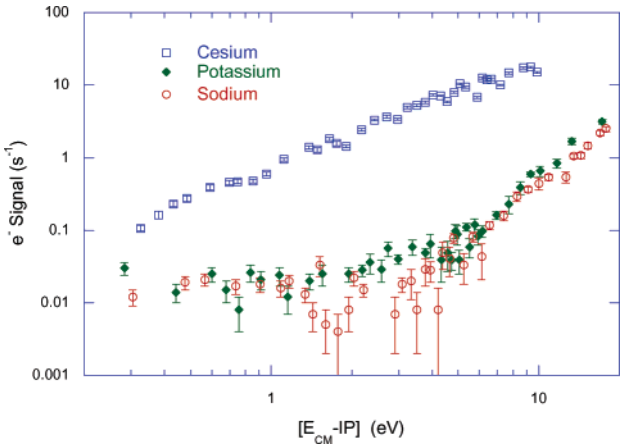

Figure 4. Electron signal rates for HV on, positive end attack versus energy above ionization potential for the three alkali metals.

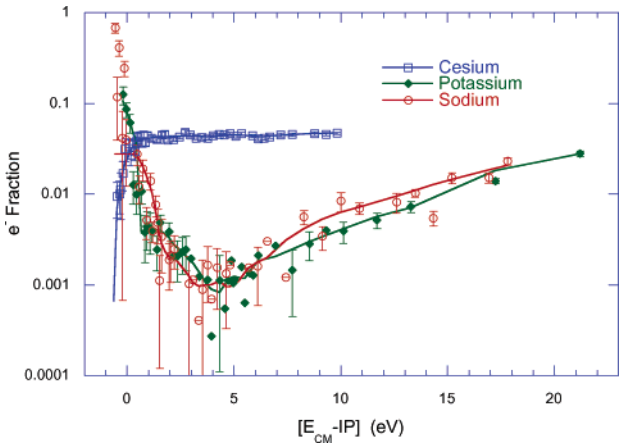

Figure 5. Fraction of signal due to electrons plotted versus energy above the alkali metal ionization potential. Signals are those for negative end attack with HV on, and curves are smooth fits to the data.

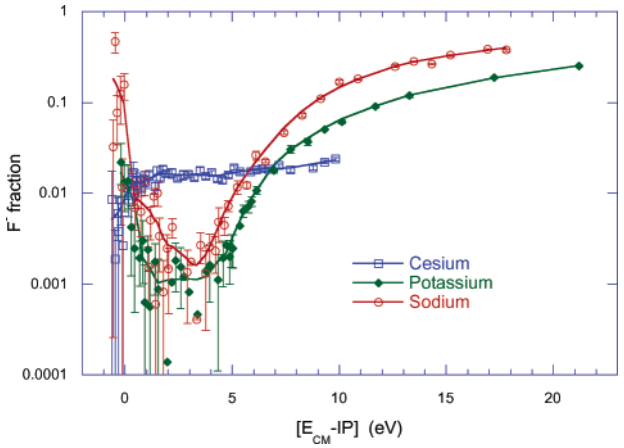

Figure 6. Fraction of ions due to F^- plotted versus energy above the ionization potential of the various alkali metals for negative end attack with HV on. Curves are smooth fits.

negative end attack; positive end attack data are similar and omitted for clarity. The fractions of Br^- are essentially 1.

Apparent Thresholds. Electrons and F^- ions seem to be made in different processes in cesium, and the apparent thresholds for these two ions appear vastly different from those for potassium or sodium. This is shown in Figures

7 and 8 for positive end attack; negative end attack signals are similar and omitted for clarity. Apparent thresholds are

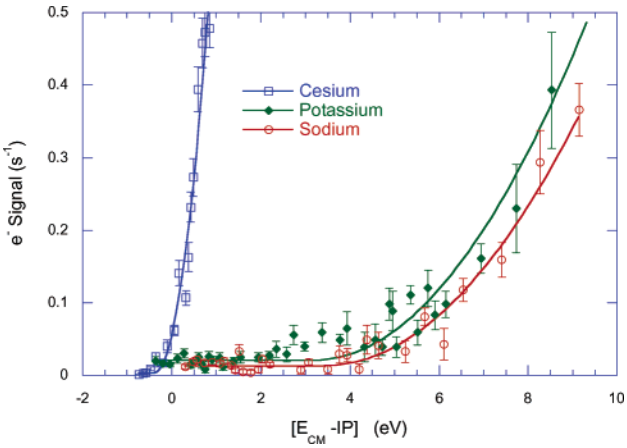

Figure 7. Electron signals rates versus energy above the alkali metal ionization potential for positive attack geometries for the various alkali metals. Curves are fits to the data described in the text.

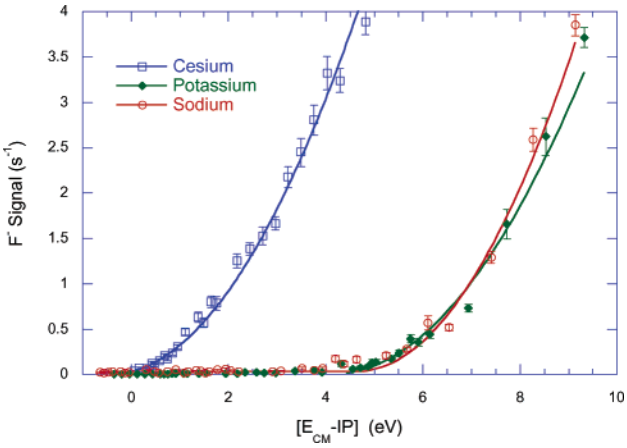

Figure 8. Fluoride ion signal rates for positive attack geometries for the various alkali metals plotted versus energy above the ionization potential. Curves are fits to the data as described in the text.

obtained by fitting the data to the same quadratic functional form used to fit the Br^- signals for energy calibration and are collected in Table 1. The energy scale for each alkali metal is calibrated using the threshold for the Br^- ions, but the thresholds for F^- show interesting deviations from those expected.

For Cs, the electron threshold is roughly correct and adds credence to the calibration procedure, but the F^- threshold appears low. This apparent low threshold probably results[37] from reaction of Cs_2 to produce $CsBr + Cs^+ + F^- + CF_2$ which would give a Cs^+/F^- coincidence signal and is expected to have a threshold of ca. 3.1 eV,[38] close to that observed. On the other hand, for sodium and potassium, the experimental F^- thresholds are some 2 eV too high, and the experimental thresholds for electron formation are about 3 eV too high. Although each threshold is probably uncertain to about 0.5 eV, these values suggest that sodium and potassium have some energy barrier to reaction, leaving the products in excited states. (The errors shown in parentheses reflect the difference between positive and negative end attack.)

(36) Radzig, A. A.; Smirnov, B. M. *Reference Data on Atoms, Molecules, and Ions*; Springer: Berlin, 1985.
(37) Reck, G. P.; Mathur, B. P.; Rothe, E. W. *J. Chem. Phys.* **1977**, *66*, 3847−3853.
(38) *NIST Chemistry WebBook*; NIST Standard Reference Database Number 69, 2003.

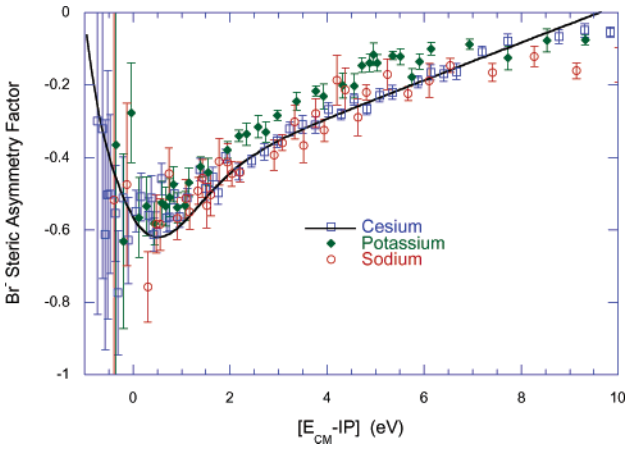

Figure 9. Steric asymmetry factor for Br^- versus energy above the alkali metal ionization potential. The positive end of the molecule is more reactive for all points. The curve is fit to the cesium data using a model assuming that reactivity arises from separate low-energy and high-energy processes.

Table 2. Model Parameters

	Cs–Br	Cs–F	K–F
a_+^L	150	0.1	150
b_+^L	400	0.4	5
a_-^L	150	0.1	5
b_-^L	400	0.3	900
a_+^H	300	300	100
b_+^H	−10	7	10
a_-^H	100	7	190
b_-^H	11	37	8
c	2	2	1
E_H	4	3.5	9
E_L	2.9	3.4	8.4

Steric Effects. Figure 2 shows that the positive (Br) end of the CF_3Br molecule is more reactive to form Br^-. The overall cross section for ion formation increases dramatically with energy, and we wish to focus on the effect of orientation and de-emphasize the energy variation of the overall cross section. We thus compute the steric asymmetry factor, defined as

$$G = \frac{\sigma_- - \sigma_+}{\sigma_- + \sigma_+}$$

Here, $\sigma_\pm$ is the cross section for reaction in the positive/negative orientation. If reactivity is the same at either end, $G = 0$, but if only one end of the molecule is reactive, $G = \pm 1$, depending on which end is reactive. Thus, G must lie between -1 and $+1$.

Figure 9 shows the steric asymmetry for formation of the most abundant ion, Br^-, plotted versus $(E_{CM} - E_0)$, the energy above the Br^- threshold. Once the price of transferring the electron has been paid, the various alkali metals show essentially the same steric asymmetry. The curve is a multiparameter model fit to the Cs data that assumes reactivity arises from two channels, a low-energy channel favoring the negative end, and a higher-energy channel favoring the positive end.[35] The parameters are determined by trial and error and are shown in Table 2.

In previous work on *tert*-butyl bromide and CF_3H, we found that the steric asymmetry apparently reverses at energies near threshold. Figure 9 suggests that the steric asymmetry factor, G, is minimizing at energies very close to the threshold. The steric asymmetry is calculated from separate measurements of reactivity at the positive end and negative end. These measurements suggest that G may reverse sign here as well.

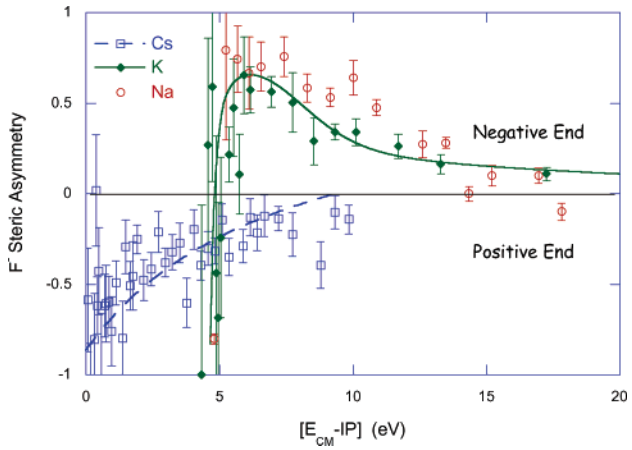

Figure 10. Steric asymmetry factors for F^- plotted versus energy above the alkali metal ionization potentials. The curves are model fits to the cesium and potassium data.

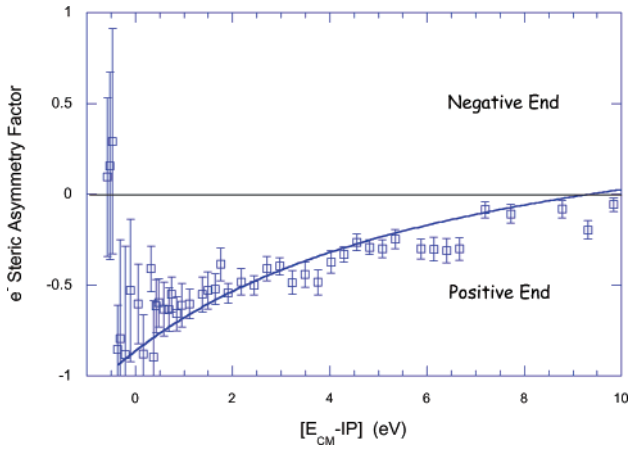

Figure 11. Steric asymmetry factor for electrons from cesium. The curve is obtained for the F^- steric asymmetry data for cesium.

The steric asymmetry for formation of F^- is completely different from that for Br^- and is shown in Figure 10. Cesium produces F^- down to low energies, and the positive end of the molecule is always more reactive than the negative end. Potassium and sodium, on the other hand, favor the negative end of the molecule at energies a few volts above the ionization potential (IP). The steric asymmetry maximizes ~6 eV above the IP and then appears to change sign as the energy is decreased. To within the uncertainty in the data, sodium and potassium appear to behave identically. The curves shown are multiparameter fits similar to that shown in Figure 9.

Figure 11 shows the steric asymmetry for electrons resulting from cesium attack. The electrons show a strong preference for positive end attack, and the steric asymmetry is apparently identical to that observed for F^-. The curve in Figure 11 is the same curve calculated to fit the F^- steric asymmetry shown in Figure 10. Electron data for sodium and potassium are wildly scattered and inconclusive because the signals are so low. The signals for the parent negative ion were too low to analyze.

IV. Discussion

Several authors have studied electron-transfer processes similar to those reported here, especially at higher energies, and

much of our interpretation relies on their groundwork.[16−18,20,39−41] The events seem to be fairly well described in terms of the Landau−Zener curve-crossing theory, especially if allowance is made for the role of extra dimensions introduced by the internal coordinates of the molecules involved.

CF_3Br attaches both free and bound electrons,[11,20,25,39,42−46] apparently making it extraordinarily effective as a fire-extinguishing agent. The parent negative ion, CF_3Br^-, is stable with an elongated C−Br bond[47] and EA of 0.91 eV.[20] Electron-scattering experiments[45] show resonances in CF_3Br at ∼1.5 and 4.5 eV, the former a little lower in energy than that for CF_3Cl.[45,48]

Both experiment and theory show that the LUMO in CF_3Br is the σ^*_{CBr} orbital, and the next higher orbital seems to be CF antibonding. For the related compound, CF_3Cl, electron-scattering resonances[45,49] are observed near 2.0, 5.5, and 8.5 eV. These broad features are signatures of very short-lived transient negative ions that decay by ejection of an electron (autodetachment) or by the breaking of a chemical bond. Thus, Cl^- is observed[42,46] at energies of ∼1.3 eV (and 5 eV) and F^- is observed at ∼4 eV, a little lower than the nominal energy of the resonance because autodetachment dominates at higher energy. Electron energy loss measurements[48] show that the ν_3 CCl stretch is excited near 2 eV and that the ν_1 and ν_4 CF_3 stretches are excited near 5 eV. The lowest resonance (2 eV) is assigned to an a_1 σ^*_{CCl} orbital, and higher resonances at 5.5 and 8.5 eV were assigned to e and a_1 symmetries corresponding to antibonding CF orbitals.

Electron energy loss data are not available for CF_3Br, but dissociative attachment forms Br^- and F^- at energies slightly lower than the electron resonances. The energy of the lowest resonance decreases as Cl → I, showing that the LUMO is associated with the unique halogen. The higher resonance is relatively unchanged, suggesting that the higher energy resonance is associated with CF_3. The electron-scattering data and more recent calculations[47] thus agree that the LUMO (responsible for the lowest resonance) is σ^*_{CBr}. The resonances at somewhat higher energies responsible for production of F^- involve an antibonding CF orbital, assigned as σ^*_{CF} by Mann and Linder[48] and as π^*_{CF} by Underwood et al.[45]

Comparison of Alkali Metals. Figure 9 shows that the steric asymmetry for production of Br^- by electron transfer from any of the three alkali metal atoms is basically the same, provided allowance is made for the ionization potential of the atom. This overall agreement engenders some confidence in the energy calibration procedure.

The steric asymmetry is large and Br^- formation is most likely if the Br end of the molecule is attacked, consistent with the inbound electron entering the σ^*_{CBr} LUMO. Although the electron-scattering data suggest that higher lying orbitals could become important at higher energies, these are not expected to play a role here. The two-channel model used to fit the steric asymmetry probably reflects different behavior in the final escape of the ions. The trend in the steric asymmetry suggests that at very low energies (where only the σ^*_{CBr} LUMO is accessible) Br^- production might be preferred for attack at the CF_3 end. It is reminiscent of previous work in CF_3H and *tert*-butyl bromide where the "backside" approach was more effective at low energies, apparently because direct attack at low energies is more likely to produce salt molecules (which are not detected) rather than separated ions. Previous potassium experiments at thermal energies, where the only possible product is the salt, have shown that the salt (KBr) is scattered at different angles, depending on the initial orientation, with Br end attack being about twice as reactive as CF_3 end attack.[50] This was rationalized by suggesting that the electron might be transferred more easily at the Br end, followed by prompt ejection of the Br^- along the direction of orientation. The present data suggest that the electron is indeed preferentially transferred at the Br end.

The almost boring commonality of the various donors for bromide ion formation is broken for fluoride formation. Virtually all of the data shown (Figures 3−6 and Figure 10) reinforce the notion that the reactivity of cesium is different from that of sodium or potassium. Because of the lower ionization potential of cesium, the electron should be transferred at longer range than that for either sodium or potassium. At larger distances, there is less interaction between the nascent ions, and in the limit of zero ionization potential (i.e., a high Rydberg atom) the electron would be equivalent to a free electron.[23] Thus, for cesium, the electron may be "quasi-free", and the decomposition of the transient CF_3Br^- negative ion might be expected to be independent of the Cs^+ core. Figures 5 and 6 show that the fraction of fluoride ions and the fraction of electrons is essentially independent of the cesium atom's energy. The fraction of electrons formed in cesium collisions is about 2 orders of magnitude greater than that for potassium or sodium, suggesting that the transient negative ion formed by potassium or sodium is stabilized with respect to autodetachment. For cesium, the steric asymmetry for formation of fluoride and for the free electron (Figures 10 and 11) shows that all of the negative ions formed favor transfer at the positive end of the molecule. All in all, the transient negative ion is not affected very much by the Cs^+ core ion.

Sodium and potassium are similar but behave differently from cesium. Although there seems to be minimal interference of the Cs^+ ion core in the decomposition of the transient CF_3Br^- negative ion, the lighter alkali metals affect the formation and decomposition. The apparent thresholds for formation of F^- and e^- are about 4 eV higher than the corresponding thresholds with cesium, and several eV above the minimum required to form F^- or electrons. This apparently reflects an energetic barrier to reaction. In addition, there are enormous qualitative differences in the steric asymmetry for fluoride formation: the positive end is favored for cesium, but the negative end is favored for potassium and sodium.

(39) Rothe, E. W.; Tang, S. Y.; Reck, G. P. *Chem. Phys. Lett.* **1974**, *26*, 434−6.
(40) Baede, A. P. M. *Adv. Chem. Phys.* **1975**, *30*, 463−535.
(41) Kleyn, A. W.; Moutinho, A. M. C. *J. Phys. B: At. Mol. Opt. Phys.* **2001**, *34*, R1−44.
(42) Illenberger, E.; Scheunemann, H.-U.; Baumgärtel, H. *Chem. Phys.* **1979**, *37*, 21−31.
(43) Hasegawa, A.; Shiotani, M.; Williams, F. *Faraday Discuss. Chem. Soc.* **1978**, *63*, 157−174.
(44) Xing, G. *Orientation Effects in Cross Beam Ionization Reactions between Potassium and Symmetric-top Molecules*; Rice University: Houston, 1993.
(45) Underwood-Lemons, T.; Winkler, D. C.; Tossell, J. A.; Moore, J. H. *J. Chem. Phys.* **1994**, *100*, 9117−22.
(46) Underwood-Lemons, T.; Gergel, T. J.; Moore, J. H. *J. Chem. Phys.* **1995**, *102*, 119−23.
(47) Roszak, S.; Koski, W. S.; Kaufman, J. J.; Balasubramanian, K. *J. Chem. Phys.* **1997**, *106*, 7709−13.
(48) Mann, A.; Linder, F. *J. Phys. B* **1992**, *25*, 1621−32.
(49) Jones, R. K. *J. Chem. Phys.* **1986**, *84*, 813−19.
(50) Carman, H. S.; Harland, P. W.; Brooks, P. R. *J. Phys. Chem.* **1986**, *90*, 944−8.

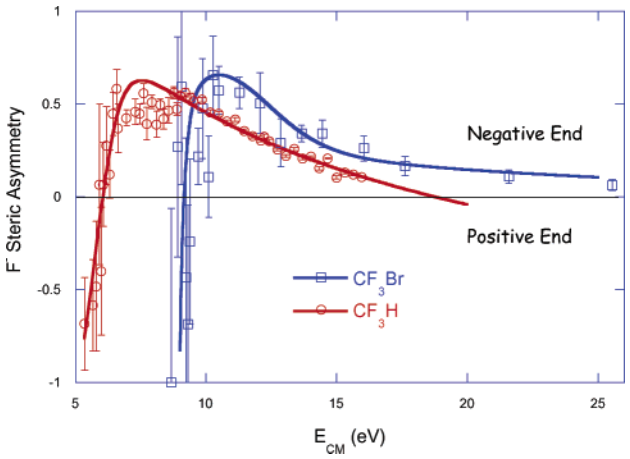

Figure 12. Comparison of F^- steric asymmetry for potassium reacting with CF_3H and CF_3Br. Curves are fits calculated using the model discussed in the text. Abscissa is E_{CM}.

By virtue of their higher ionization potentials, the lighter alkali metals must approach more closely before the electron is transferred, and the positive ion is expected to play a more active role in the reaction, as is observed. Figure 5 shows that the fraction of electrons produced in Na and K collisions is far lower than that observed in Cs collisions. Apparently, the closer proximity of the Na and K ions relaxes[51] the transient CF_3Br^- negative ion, elongating the C−Br bond, possibly favoring the formation of the parent negative ion at the expense of Br^- formation.[47]

Fluoride ions are apparently not formed from sodium or potassium via the σ^*_{CBr} LUMO. The Br^- steric asymmetry shows that electrons are more likely to enter this orbital at the Br end of the molecule. Attack at the Br end would prepare the nascent M^+ and F^- ions at maximum separation, which would minimize the chances of their recombining to give a salt molecule, and thus maximize F^- formation. This is evidently happening with cesium, where the Br end is more reactive. Yet sodium and potassium react at the CF_3 end and thus make participation of the σ^*_{CBr} LUMO unlikely. Instead, the electron apparently enters a higher antibonding CF orbital, analogous to the orbitals in CF_3Cl responsible for excitation of the CF_3 stretching vibrations described earlier.[48] This higher energy orbital is apparently restricted to shorter-range electron transfer and accounts for the energy barrier observed. The larger cesium atom is apparently unable to access this orbital, perhaps because the electron has already been transferred to the σ^*_{CBr} orbital at larger range. Sodium, on the other hand, has the highest ionization potential of the donors studied and is expected to transfer its electron at the shortest range where the CF orbital is most accessible. As Figure 6 shows, sodium produces the greatest fraction of F^-.

Comparison to Other Molecules. Figure 12 compares the F^- steric asymmetry for potassium reacting with CF_3Br and CF_3H.[52] The steric asymmetry for F^- for each of these compounds is very similar, except that CF_3Br is moved to higher energy by about 3 eV. (We regard the kink in the CF_3Br curve near 15 eV as a meaningless artifact of the fit.) For both molecules, fluoride formation is favored upon CF_3 end attack, and the maximum steric asymmetry of ∼0.6 indicates that the CF_3 end orientation is about 4 times more reactive (to form F^-) than the Br end orientation.

In CF_3H, the F^- signal is far higher than that in CF_3Br, ending the similarity. In CF_3H, the LUMO is σ^*_{CH}, and at very low energies the electron is transferred at the H end of the molecule to produce nascent ions as widely separated as possible, making them easier to escape their Coulomb attraction. As the energy is raised, the higher energy σ^*_{CF} orbital becomes available and the additional energy enables the ions to be separated, both factors favoring a shift to the CF_3 end approach.

In CF_3Br, of course, the LUMO is σ^*_{CBr}, and electron transfer to this orbital favors the formation of Br^-, a channel simply not available in fluoroform. Even for CF_3 end attack, Br^- is the major product in CF_3Br as shown by Figure 6. Attack at the CF_3 end of the molecule apparently allows the electron to enter an orbital described partially as σ^*_{CBr}, making formation of Br^- still possible. The CF antibonding orbital(s) become available at higher energy, and F^- begins to be produced. The apparent threshold for F^- production is about 3 eV higher than expected (Table 1) and roughly corresponds to the energy between electron resonances.[46] The extra energy required to produce F^- (∼3 eV) is almost exactly the energy required to break the C−Br bond,[53] so the apparent F^- threshold might correspond to production of M^+, F^-, Br^0, and CF_2, where M = Na or K. An event like this could conceivably lead to production of a mixed halogen anion (XY^-), observed in electron attachment experiments.[54]

V. Summary

Three alkali metal atoms (sodium, potassium, and cesium) are studied to investigate the effects of varying the electron donor in an electron transfer with CF_3Br. Positive end (Br end) attack preferentially forms the most abundant negative ion, Br^-, and all three donors behave similarly. Apparently, the σ^*_{CBr} LUMO is most accessible to the incoming electron at the Br end of the molecule, rather than inside the CF_3 umbrella.

Cesium attack also produces small amounts of fluoride ion, F^-, and free electrons, again at the positive (Br) end of the molecule. Yet if the donor is sodium or potassium, fluoride formation is completely different. The apparent energetic threshold is significantly higher, and fluoride formation is favored at the negative (CF_3) end of the molecule. Cesium has the lowest ionization potential of the three donors, and its electron appears to be transferred (to the positive end of the molecule) at a distance large enough that the Cs^+ ionic core does not affect the decomposition of the transient CF_3Br negative ion. Fluoride ions are apparently produced from sodium and potassium by short-range transfer to an antibonding CF orbital a few eV above the LUMO.

Acknowledgment. We gratefully acknowledge the financial support of this research that has been received from the Robert A. Welch Foundation and the National Science Foundation.

JA036451B

(51) Zembekov, A. A. *Chem. Phys. Lett.* **1971**, *11*, 415−6.
(52) Jia, B.; Laib, J.; Lobo, R. F. M.; Brooks, P. R. *J. Am. Chem. Soc.* **2002**, *124*, 13896−13902.
(53) McMillen, D. F.; Golden, D. M. *Annu. Rev. Phys. Chem.* **1982**, *33*, 493−532.
(54) Ingolfsson, O.; Weik, F.; Illenberger, E. *Int. J. Mass Spectrom. Ion Processes* **1996**, *155*, 1−68.